Afyon Kocatepe Üniversitesi Fen ve Mühendislik Bilimleri Dergisi
Afyon Kocatepe University – Journal of Science and Engineering
https://dergipark.org.tr/tr/pub/akufemubid

Araştırma Makalesi / Research Article
e-ISSN: 2149-3367
DOI: https://doi.org/10.35414/akufemubid.1660346
AKÜ FEMÜBİD **25** (2025) 065203 (1386-1398)
AKU J. Sci. Eng. **25** (2025) 065203 (1386-1398)

Comparative Analysis of Bidirectional Totem-Pole and Interleaved Totem-Pole PFC Converters for Level 2 Electric Vehicle Chargers

Makale Bilgisi / Article Info
Alındı/Received: 18.03.2025
Kabul/Accepted: 15.07.2025
Yayımlandı/Published: 03.12.2025

Seviye 2 Elektrikli Araç Şarj Cihazları İçin Bidirectional Totem-Pole ve Interleaved Totem-Pole PFC Dönüştürücülerinin Karşılaştırmalı Analizi

Marwan HAMAD* **and Yunus YALMAN**

Ankara Yıldırım Beyazıt Üniversitesi, Mühendislik ve Doğa Bilimleri. Fak., Elektrik Elektronik Müh. Böl. Ankara, Türkiye

Abstract

The global trend toward electrification is significantly accelerating the adoption of electric vehicles (EVs), making the development of efficient and grid-friendly charging solutions a critical research priority. Among these solutions, bidirectional chargers play a vital role in minimizing the impact on the electrical grid by ensuring low total harmonic distortion (THD), a high-power factor (PF), enabling vehicle-to-grid (V2G) functionality. This paper presents a comparative analysis of two advanced topologies of single-phase totem-pole power factor correction (PFC) converters designed for Level 2 EV chargers, operating at a rated voltage of 230 Vrms and power levels of up to 18 kW. Specifically, a bidirectional totem-pole converter and a bidirectional interleaved totem-pole converter are evaluated based on key performance metrics, including THD, PF, and efficiency under both steady-state and transient conditions. The simulation results indicate that both topologies achieve high efficiency and near-unity power factor. However, the interleaved topology exhibits superior performance in minimizing THD and managing high-power conditions while maintaining low current stress on the switches. Nonetheless, this configuration presents a trade-off, resulting in a higher output voltage ripple compared to the standard totem-pole configuration. At 18 kW, the totem-pole converter achieves a THD of 1.72% and an efficiency of 98.1%, while the interleaved totem-pole converter demonstrates improved performance with a THD of 1.14% and an efficiency of 98.6%.

Keywords: *Electric Vehicles (EVs); Bidirectional Totem-Pole PFC Converters; Vehicle to Grid (V2G); Level 2 EV Charger.*

Öz

Küresel ölçekte elektrifikasyona yönelik eğilim, elektrikli araçların (EV) benimsenme hızını önemli ölçüde artırmakta ve şebeke dostu, yüksek verimli şarj çözümlerinin geliştirilmesini kritik bir araştırma alanı haline getirmektedir. Bu bağlamda, çift yönlü şarj cihazları, düşük toplam harmonik bozulma (THD) ve yüksek güç faktörü (PF) sağlayarak, aynı zamanda araçtan şebekeye (V2G) enerji aktarımını mümkün kılarak, elektrik şebekesi üzerindeki olumsuz etkileri en aza indirmede önemli bir rol oynamakta-dır.Bu çalışma, 230 Vrms nominal gerilimde ve 18 kW'a kadar güç seviyelerinde çalışan Seviye 2 EV şarj istasyonları için tasar-lanmış iki farklı gelişmiş tek fazlı totem-pole güç faktörü düzeltme (PFC) dönüştürücü topolojisinin karşılaştırmalı ana-lizini sunmaktadır. Özellikle, çift yönlü totem-pole dönüştürücü ile çift yönlü interleaved totem-pole dönüştürücü ele alınarak, söz konusu yapıların kararlı ve geçici durum koşullarında toplam harmonik bozulma (THD), güç faktörü (PF) ve verimlilik açısından performansları değerlendirilmekte dir.Simülasyon sonuçları her iki dönüştürücü topolojisinin de yüksek verimlilik ve birim de-ğere yakın güç faktörü sağladığını doğrulamaktadır. Özellikle interleaved totem-pole topolojisi, toplam harmonik bozulmayı (THD) azaltma ve yüksek güçlü çalışma koşullarını yönetme konusunda üstün performans sergilemekte; aynı zamanda anahtarlama elemanları üzerindeki akım zorlanmasını da azalt-maktadır. Ancak, bu topoloji belirli bir ödünleşim içermekte olup, geleneksel totem-pole konfigürasyonuna kıyasla daha yüksek çıkış gerilimi dalgalanması göstermektedir. 18 kW çıkış gücünde, standart totem-pole dönüştürücü %1,72 THD ve %98,1 verimlilik sağlarken; interleaved yapı %1,14 THD ve %98,6 verimlilik ile daha iyi bir performans ortaya koymaktadır.

Anahtar Kelimeler: *Elektrikli Araçlar (EV'ler); Çift Yönlü Totem-Kutup PFC Dönüştürücüler; Araçtan Şebekeye (V2G); Seviye 2 EV Şarj Cihazı.*

1. Introduction

The rapid widespread adoption of EVs, driven by their enhanced reliability and environmentally friendly characteristics, continues to gain momentum today (Meetly et al. 2020). Bidirectional EV chargers facilitate power transfer in two directions: from the grid to the vehicle's battery (Grid-to-Vehicle, or G2V) and from the vehicle's battery back to the grid (V2G). These chargers can be classified into two configurations based on the number of stages involved: 1) single-stage configuration (Sayed et al. 2018) and 2) two-stage configuration. The two-stage configuration is notably the more prevalent choice, consisting of a PFC stage and a DC-DC conversion stage. The popularity of the two-stage configuration can be attributed to its implementation of galvanic isolation in the DC-DC stage and the ease of control for the separate stages (Asmatullah et al. 2022, Upturn and Subuddhi 2024).

*Sorumlu Yazar/Corresponding Author: Marwan Hamad e-posta / e-mail: m.n.t.hamad23@aybu.edu.tr

The EV chargers can be also classified into three levels based on their power rating and the charging speed. A Level 1 charging system (<1.9 kW) uses a single-phase 110/120 Vrms supply with a maximum current of 12 A. Level 2 systems (<19.2 kW) can operate on single-phase 230 Vrms, offering output powers of 3.6 kW, 7.2 kW, or 19.2 kW, or on three-phase configurations. Level 3 systems (<100 kW) are exclusively three-phase (Yilmaz and Kreon 2013). Future developments are mainly focused on Level 2, which is a semi-fast charging system that offers significant power capacity and can be customized for various environments, suitable for both private and public facilities (Int. Ref.-4,Int. Ref.-2).

To address power quality issues in two stages of EV chargers, the front-end stage, commonly known as the PFC stage, plays a crucial role. There are various topologies proposed in the literature for the PFC stage, which can generally be classified into two categories: bridge PFC converters and bridgeless PFC converters. Bridge PFC converters, like the boost PFC topology regards as the most popular topology under this classification, have certain limitations, such as not supporting bidirectional power flow or facing challenges during reverse operation. This is particularly relevant as the trend shifts towards bidirectional EV chargers (BEVCs), especially with the increasing integration of distributed generation sources (DGs) into the conventional grid system. This shift has amplified the need for BEVCs to effectively integrate with various DGs and enhance the reliability of the grid. Additionally, bridge PFC converters incur extra losses due to the presence of the bridge compared to bridgeless PFC converters (Figueiredo, Toffoli, and Silva 2010). Consequently, Bridgeless PFC converters are regarded as one of the best options for enhancing power quality issues and boosting efficiency (Singh and Tiwari 2020).

While bridge-based PFC converters are unsuitable for bidirectional BEVCs, various topologies fall under the category of bridgeless PFC converters. Among these, the dual boost bridgeless PFC converter is a widely adopted topology; however, it produces significant common-mode noise, requiring a large electromagnetic interference (EMI) filter (Ye et al. 2004, Lu, Brown, and Sodano 2005, Kong, Wang, and Lee 2007). Address the limitations of earlier bridgeless PFC designs, alternative topologies such as the semi-boost bridgeless PFC converter (Mousavi, Eberle, and Dunford 2011) and the pseudo totem-pole bridgeless PFC converter (Huber, Jang, and Jovanović 2008) have been proposed in the literature.

One significant type of bridgeless topology among various bridgeless boost PFC converters is the totem-pole PFC converter (Surendra Reddy et al. 2024, Pridoli, Šupolík, and Praženica 2025), as illustrated in Figure 1(a). This topology presents several advantages, including a reduction in component count, a compact form factor, diminished common mode interference, and the ability to achieve both high power density and efficiency (Li and Nui 2024, ,Park et al. 2019). Recent modifications to the conventional totem-pole boost PFC converter, specifically the replacement of the two diodes on the right leg with low-frequency MOSFETs and the two MOSFETs on the right leg with wide bandgap (WBG) MOSFETs, have gained considerable attention in high-power applications, such as EV chargers (Zhou et al. 2015). These advancements position totem-pole PFC converters as one of the most advanced and optimized topologies in the development of bridgeless PFC converters, as proposed in the literature, to overcome the limitations of other bridgeless designs while achieving superior efficiency(Liu et al. 2015, Ghosh, Hu, and Batash 2023).

Numerous totem-pole topologies have been investigated for EV charging applications; however, most studies concentrate on unidirectional or lower power scenarios, typically below 10 kW (Tang, Ding, and Khaligh 2016, Kumar and Yi 2022). Furthermore, there is a lack of comparative research on the dynamic and steady-state power quality performance of interleaved versus non-interleaved configurations in single-phase high-power applications. This paper aims to address this gap by simulating and evaluating both bidirectional totem-pole and interleaved totem-pole PFC converters under high-power conditions (up to 18 kW) typical of Level 2 EV charging. The focus will be on practical grid compliance metrics, including THD, PF, and output ripple.

The objective of this paper is to conduct a comparative study of two single-phase totem-pole PFC converters based on WBG devices, such as Sic, designed for a Level 2 EV charger operating at a rated voltage of 230 Vrms and a power level of up to 18 kW. The study focuses on two configurations: the bidirectional totem-pole converter and the bidirectional interleaved totem-pole converter. The comparison evaluates key performance metrics, including power quality aspects such as THD and PF, as well as efficiency. Both converters are analyzed under steady-state and transient operating conditions.

The paper is structured as follows: Section II provides an overview of the two converter topologies and the associated control methods. Section III presents the simulation results, while Section IV discusses the comparative analysis of the two configurations. Finally,

Section V concludes the paper with key findings and insights.

2. Theoretical Background

The initial phase of conventional EV chargers, specifically the PFC stage, is crucial as it facilitates the conversion of alternating current (AC) input voltage to a regulated direct current (DC) output voltage. Furthermore, it ensures that the AC input current waveform is sinusoidal and in phase with the AC input voltage, thereby achieving a unity power factor (PF). The proposed topologies, which are bidirectional totem pole, and bidirectional interleaved totem pole topologies, are bidirectional PFC stages for EV chargers, with the results focusing on improvements in power quality, particularly in G2V applications. This section will present the theoretical foundations of two totem pole topologies, along with a detailed description of the controller.

2.1 Bidirectional Totem-Pole Topology

The totem-pole converter is a type of bridgeless PFC converter that operates as a combined boost converter. Its functioning is contingent upon the polarity of the AC source during the charging phase of the boost inductor. In each half-cycle, one of the high-frequency switches is activated while another synchronous switch from the opposite leg is engaged to establish a complete charging path. During this phase, the capacitor supplies power to the load. Conversely, during the discharge phase, the complementary high-frequency switch, along with the synchronous switch from the opposite leg, operates to release the energy stored in the inductor to the load. In this scenario, the capacitor is charged directly from the AC source. This operation enables efficient energy transfer and enhances power factor correction in the system. The comprehensive operation and design considerations of this converter are elaborated in (Dominic et al. 2024, Kumar and Yi 2022).

The traditional single-phase bridgeless totem-pole PFC configuration depicted in Figure 1(a) comprises two distinct legs; the high-frequency leg is characterized by the MOSFET switches $S_1$and S_2, whereas the low-frequency leg is represented by diodes D_1 and D_2, which operate in accordance with the line frequency.

The bidirectional totem-pole converter, as illustrated in Figure 1(b), retains the foundational structure of the conventional totem-pole. In the second leg, the integration of two low-frequency MOSFET switches, replacing the diodes, further mitigates conduction losses and enables the reverse operation necessary for effective EV charging (Huang 2017, Int. Ref.-1).

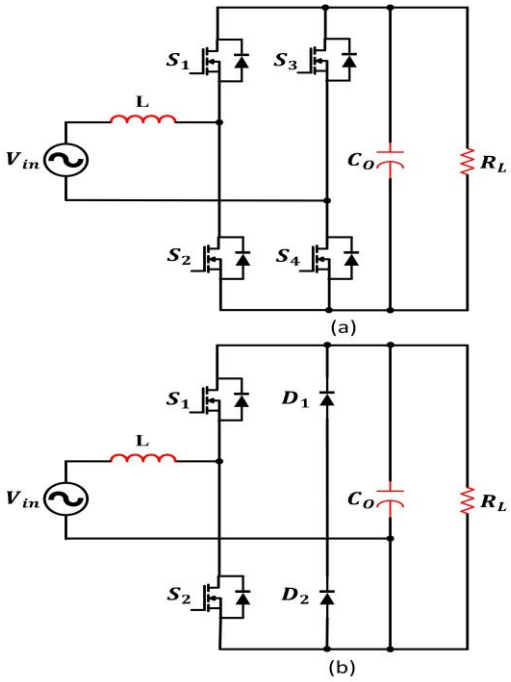

Figure 1. (a) Conventional unidirectional Totem-Pole PFC Converter. (b) Bidirectional Totem-Pole PFC Converter.

The specifications and parameter design of the proposed single-phase totem-pole PFC prototype are detailed in Table 1.

Table 1. specifications and parameter design of the proposed Totem-Pole converter.

Specifications	Value
Grid voltage (V_{in})	230 Vrms
Grid frequency (f)	50 Hz
Switching frequency (f_{SW})	100 kHz
Output voltage or DC-link Voltage (V_{dc})	400 V
Boost inductor (L)	800µH
Output Capacitor (C_O)	2500µF
Load Resistance (R_L)	(V_O^2/P_O)

2.2 Bidirectional Interleaved Totem-Pole Topology

The interleaved totem-pole PFC topology, as shown in Figure 2, consists of two boost inductors, $L_1$and L_2. Inductor $L_1$is connected to the high-frequency switching leg1, which comprises switches S_1 and S_2, while inductor L_2 is connected to the high-frequency switching leg2, consisting of switches S_3 and S_4. The third leg, known as the synchronous line-frequency leg, completes the rectification process. It employs two MOSFET switches, S_5 and S_6, in place of conventional diodes, which helps minimize conduction losses. This configuration not only enhances overall efficiency but also allows for bidirectional power flow, making it well-suited for applications that require both power factor correction and bidirectional operation. Furthermore, the interleaved design reduces input current ripple, which improves power quality and decreases the size of passive components (Int. Ref.-3).

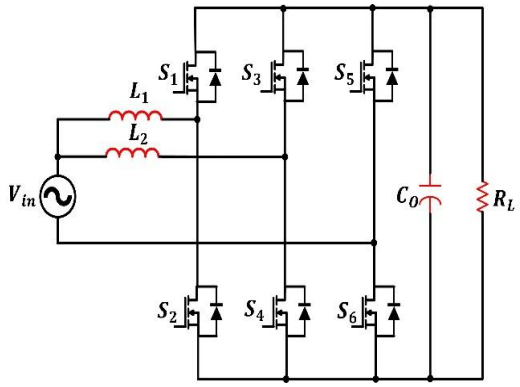

Figure 2. Proposed Bidirectional Interleaved Totem-Pole PFC Converter.

The operation of the interleaved totem-pole PFC converter is similar to the standard totem-pole topology shown in Figure 2, with a key difference: instead of using a single boost inductor, this topology employs two boost inductors. These inductors operate 180° out of phase, which reduces the input current ripple and divides the input current into two branches. This design reduces the current ratings of the switches, the size and ratings of passive components in the converter (Su and Lu 2010).

During the positive half-cycle of the AC input voltage, switches S_2 and S_4 operate at the switching frequency to charge the boost inductors. A low-frequency switch, S_6, operating at line frequency, completes the charging loop for the inductors. While the inductors are being charged, the load is supplied by the DC output capacitor. When the DC output voltage drops below the reference voltage, the controller activates another set of switches, S_1 and S_3, which are complementary to S_2 and S_4. These switches discharge the energy stored in the inductors, transferring it to the load and boosting the DC output voltage. This mode of operation is called the discharging process.

Table 2. Specifications and parameter design of the proposed Interleaved Totem-Pole converter.

Specifications	Value
Grid voltage (V_{in})	230 Vrms
Grid frequency (f)	50 Hz
Switching frequency (f_{SW})	100 kHz
Output voltage or DC-link Voltage (V_{dc})	400 V
Boost inductors (L_1&L_2)	300µH
Output Capacitor (C_O)	3000µF
Load Resistance (R_L)	(V_O^2/P_O)

Similarly, during the negative half-cycle of the AC input voltage, the converter alternates between charging and discharging the boost inductors. However, in this case, the complementary switches for each leg are used compared to those active during the positive half-cycle. For more details about the operation and design consideration of this converter are discussed in (Tang, Ding, and Khaliah 2016). The specifications and parameter design of the proposed single-phase Interleaved totem-pole PFC are detailed in Table 2.

2.3 Controller Technique

In order to effectively regulate the DC output voltage and to ensure that the input current is sinusoidal and in phase with the input voltage, it is essential to implement a closed-loop system employed in PFC converters. Various current control methodologies are employed in boost PFC converters, including hysteresis current control (Adige et al. 2022), average current control (Gupta and Vignesh Kumar, n.d.), and peak current control (Alsalem and Masoud 2024); however, the predominant technique is the average current control due to its numerous advantages, such as a straightforward control approach, resilience to external noise, reduced ripple in input current, and consistent operational stability (Jape and Musa 2009).

The control strategy proposed in this study for the two types of totem-pole PFC converter is average current control, which keeps the inductor current in continuous conduction mode (CCM). Figures 3 and 4 illustrate the control schemes of the proposed totem-pole and the interleaved totem-pole, respectively. The average current controller employed for the totem pole converters illustrated in Figure 3 makes up two control loops: an inner current loop and an outer voltage loop. Both loops use conventional Proportional-Integral (PI) control methodologies. In contrast, the controller presented in Figure 4 for the interleaved totem pole features three control loops: two inner current loops and one outer voltage loop, all of which also apply conventional PI control techniques.

The feedback control mechanism begins with the output DC voltage being measured and compared to a reference DC output voltage of 400V. The resulting error signal is then processed by a Proportional-Integral (PI) controller. The output of this voltage PI controller is scaled by a normalized input voltage to generate the inductor current reference signal (I_L*). This reference current signal is then compared to the actual measured inductor current signal (I_L), producing a new error signal that is fed into another PI controller. This controller's output decides the duty cycle for the high-frequency switches, S_1 and S_2. The duty cycle is constrained by a saturation block, ensuring it stays within the limits of 0 and 1. This duty cycle is then input into a Pulse Width Modulation (PWM) generator, which produces the necessary gate signals for the switches S_1 and S_2. This feedback control process works continuously to ensure that a sinusoidal input current is drawn, and that the DC output voltage is regulated effectively.

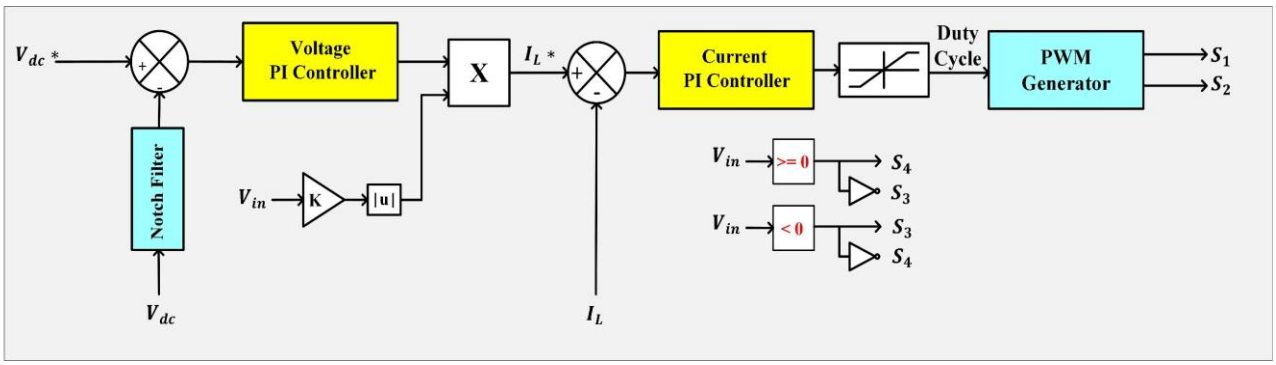

Figure 3. The average current control Scheme for the proposed Totem-Pole Converter.

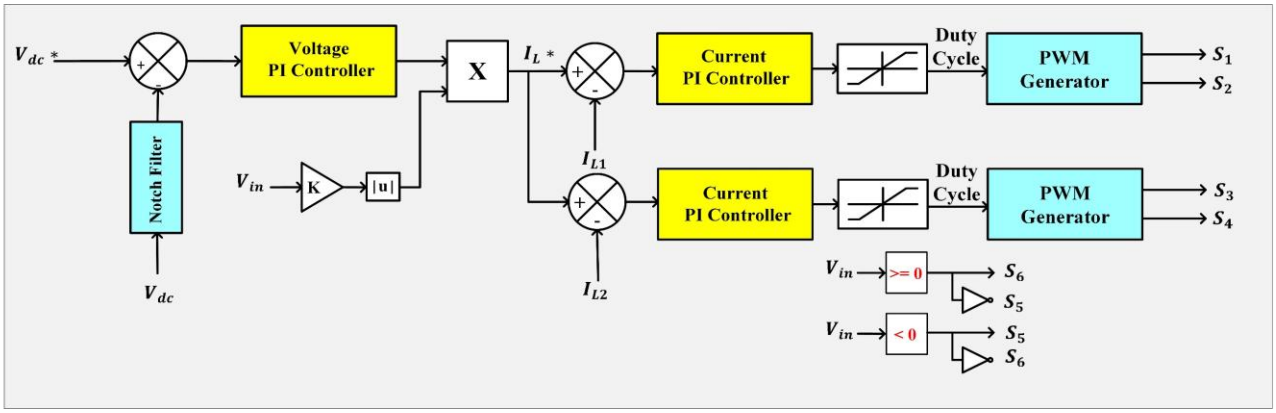

Figure 4. The average current control Scheme for the proposed Interleaved Totem-Pole Converter.

In a similar manner, the control strategy for the interleaved totem-pole converter depicted in Figure 4 follows the same principles. However, it incorporates an additional inner current control loop responsible for generating gate signals for the high-frequency switches S_3 and S_4 associated with the second leg of the converter. A distinctive feature of this control loop is that the carrier signal used in the PWM generator is phase-shifted by 180° degrees relative to the carrier signal employed in the PWM generator of the first inner current control loop. Furthermore, the pulse signals for the synchronous switches in both proposed converter configurations (namely $S_3$and S_4 for the totem-pole and S_5 and S_6 for the interleaved totem-pole converter) are generated based on the polarity of the input voltage (V_{in}). This design allows the switches to function similarly to diodes during the PFC operation of the proposed converters.

The notch filter implemented within the two control schemes illustrated in Figures 3 and 4 functions as a band-stop filter, specifically designed to attenuate the 2^{nd} order harmonic (100 Hz) ripple present in the output voltage signal. This 2nd order harmonic ripple arises as an inherent consequence of the operational characteristics of the totem pole PFC converters. The existence of harmonic significantly influences the waveform of the input current; thus, the employment of such a filter serves to mitigate power quality concerns on the input side.

2.4 Description of the Simulation

Figures 1(a) and 2 illustrate the complete configurations of the two proposed PFC converters. Both designs are intended to operate as front-end stages in single-phase onboard chargers for electric vehicles. The converters are evaluated over a wide output power range from 500 W to 18 kW, making them suitable candidates for Level 2 EV charging applications. This work proposes an alternative to conventional three-phase PFC solutions typically used at high power levels, demonstrating the feasibility of achieving high performance using single-phase topologies. The component specifications and design parameters for each converter are provided in Table 1 and Table 2, corresponding to the bidirectional totem-pole and interleaved totem-pole topologies, respectively.

The simulation models were created using MATLAB /Simulink, with all control loops implemented in a discrete-time framework. The Key simulation parameters include a nominal grid voltage of 230 Vrms at 50 Hz, a switching frequency of 100 kHz, and a regulated DC output voltage of 400 V, while maintaining the capability to expand the regulation range from 350 V to 800 V, allowing flexibility for different EV battery configurations and charging requirements. SiC MOSFETs were used as switching devices to handle the high frequency and power demands efficiently. The average current mode control strategy was applied for both converters, maintaining

CCM operation across the tested power range. The simulation time step was configured to capture 10 samples of each switching cycle, corresponding to the 100 kHz switching frequency, to accurately represent the dynamics of high-frequency switching.

3. Results and Discussions

This section discusses the simulation results of the steady-state behavior and dynamic performance of the proposed bidirectional totem pole and bidirectional interleaved totem pole topologies. The analysis covers a wide range of output power, from 500 W (light load) to 18 kW (heavy load), All voltage and current waveforms shown in the figures below are expressed in volts (V) and amperes (A).

The performance of single-phase totem pole and interleaved totem pole prototypes has been evaluated over a wide range of output power levels. Figures 5 and 6 illustrate the steady-state operation of both converters, showing their behavior under a rated 230V AC voltage during both heavy and light output power loading conditions. The simulation results indicate that the input voltage and current are in phase for both proposed PFC converters under conditions of both high and low output power, as illustrated in Figures 5(c) and 6(c) for the totem-pole prototype, and Figures 5(f) and 6(f) for the interleaved totem-pole prototype. This alignment signifies that both converters are operating at a unity power factor.

The proposed average current controllers for the two designed PFC converters effectively regulate the output DC voltage to maintain a range of 400V under varying load conditions, both high and low, as illustrated in

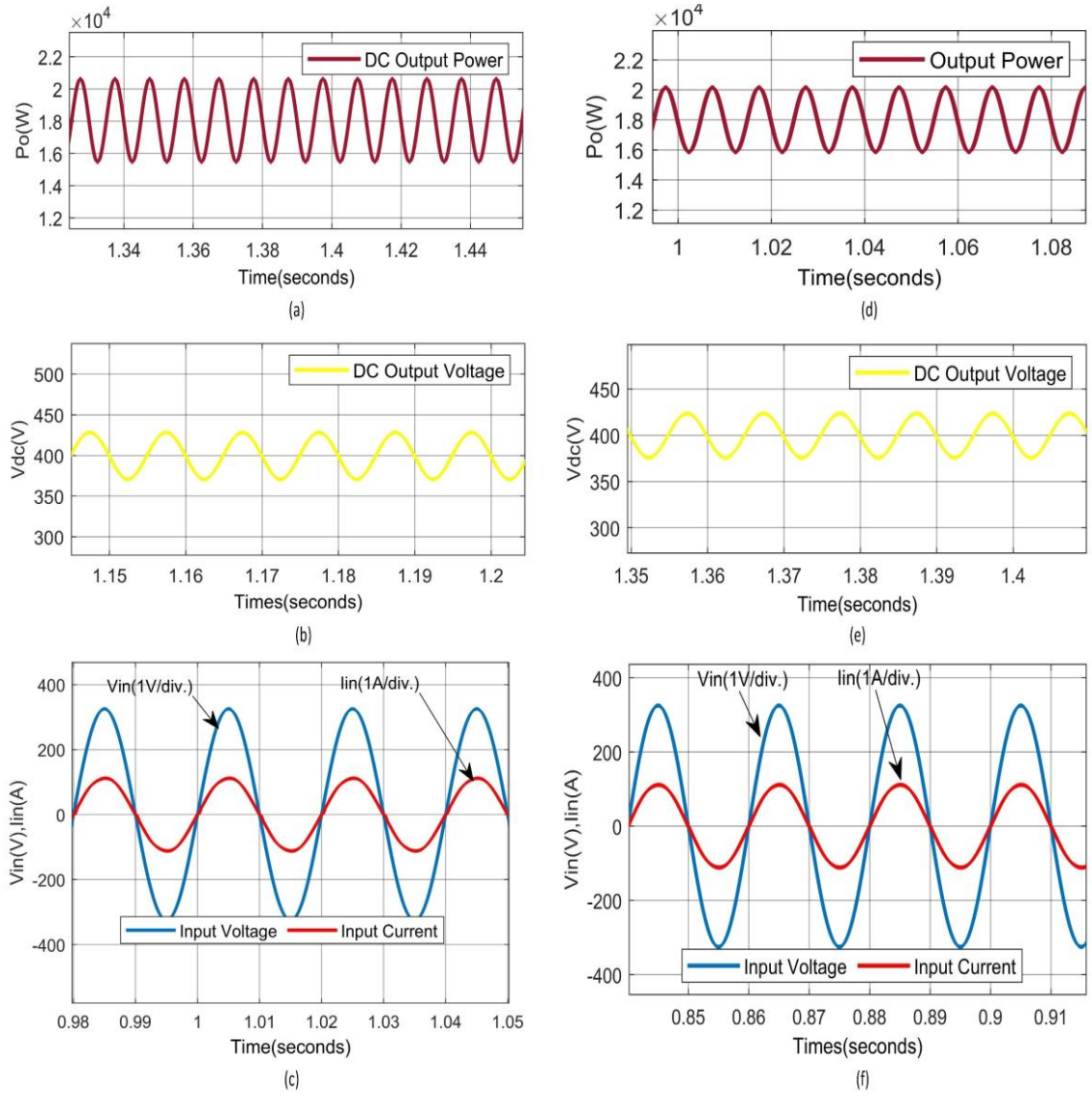

Figure 5. Steady-state input current and voltage waveforms under 18 kW load for (a–c) totem-pole and (d–f) interleaved converters, showing unity power factor operation.

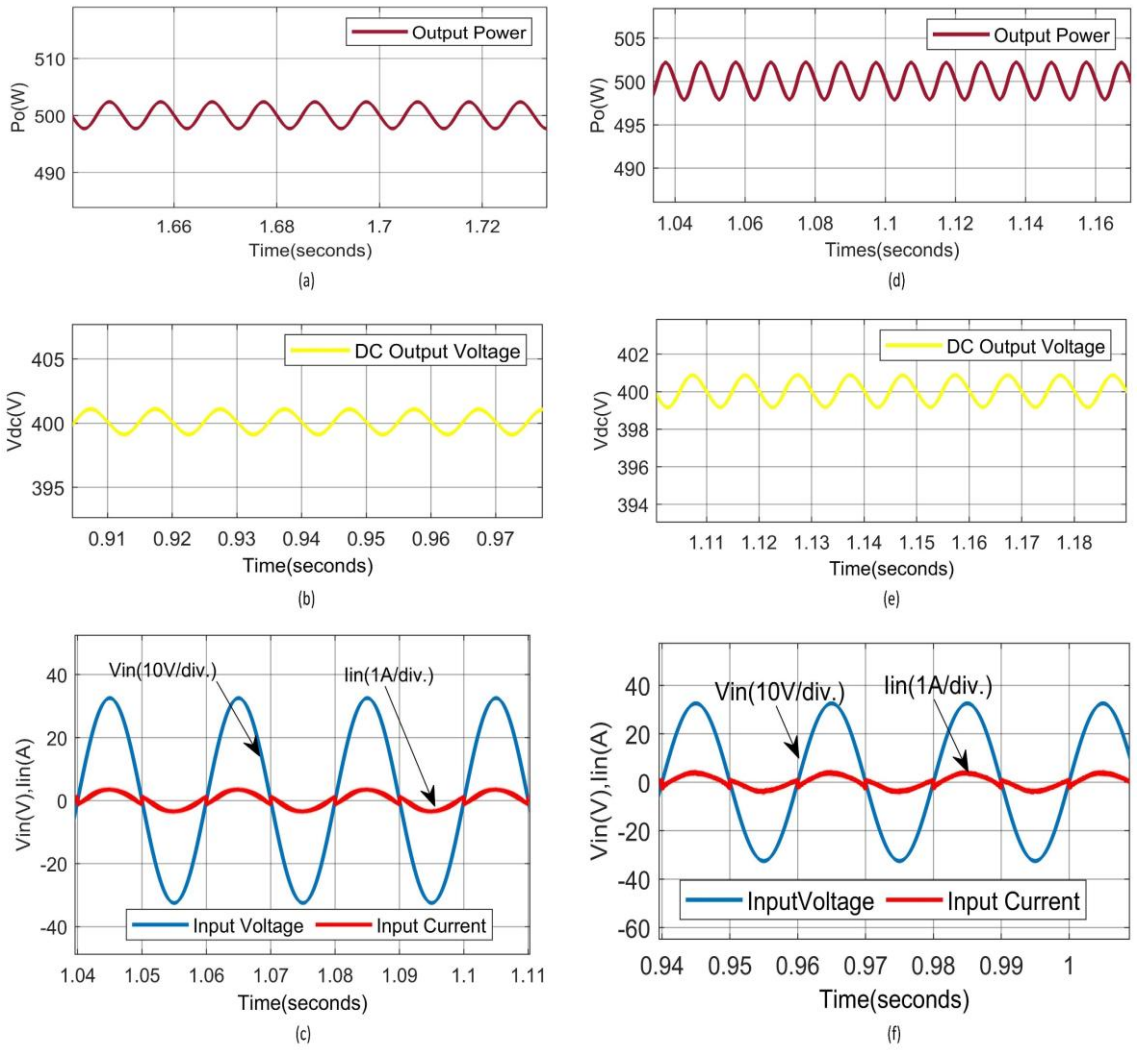

Figure 6. Steady-state input current and voltage waveforms under 500 W load for (a–c) totem-pole and (d–f) interleaved converters, showing unity power factor operation.

Figures 5(b), 6(b), 5(e), and 6(e) for both prototypes. Additionally, these controllers are capable of tracking a sinusoidal input current in accordance with the load value. Figures 5(a), 5(d), 6(a), and 6(d) depict the output power waveforms under both heavy and light load scenarios for both prototypes. Furthermore, it is noteworthy that the ripple in DC output voltage and power for the interleaved prototype is less than that observed in the totem-pole prototype.

The dynamic response of the two prototypes is evaluated under worst-case conditions, particularly during heavy load scenarios. This assessment involves subjecting the prototypes to a 20% voltage sag in the AC input voltage (down to 184 Vrms) while operating at a heavy load of 18 kW. Additionally, a 20% voltage swell in the AC input voltage (up to 276 Vrms) is applied at t = 0.8 s, maintaining the same output power load of 18 kW. The dynamic response waveforms corresponding to the sag condition for both prototypes are shown in Figure 7. During the voltage sag event, the totem-pole converter experiences a temporary drop in output power at t = 0.8 s, as shown in Figure 7(a). In response, the controller compensates by increasing the input current drawn from the grid Figure 7(c), to meet the power demand. Additionally, the DC link voltage on the output side of the converter is also affected by this sag, as depicted in Figure 7(b). The output voltage loop of the controller detects the mismatch between the desired output value and the decreased value at t = 0.8 seconds, prompting it to generate a new I_{ref} to counteract the decline in the DC link voltage. The interleaved totem-pole converter demonstrates a strong response to a 20% voltage sag. As illustrated in Figure 7(d), the output power experiences a brief dip at t = 0.8 seconds but recovers quickly as the controller increases the input current, as shown in Figure 7(f). Throughout the disturbance, the DC-link voltage stays close to the reference value of 400 V, as indicated in Figure 7(e). This stability reflects better voltage regulation compared to the single-leg totem-pole configuration.

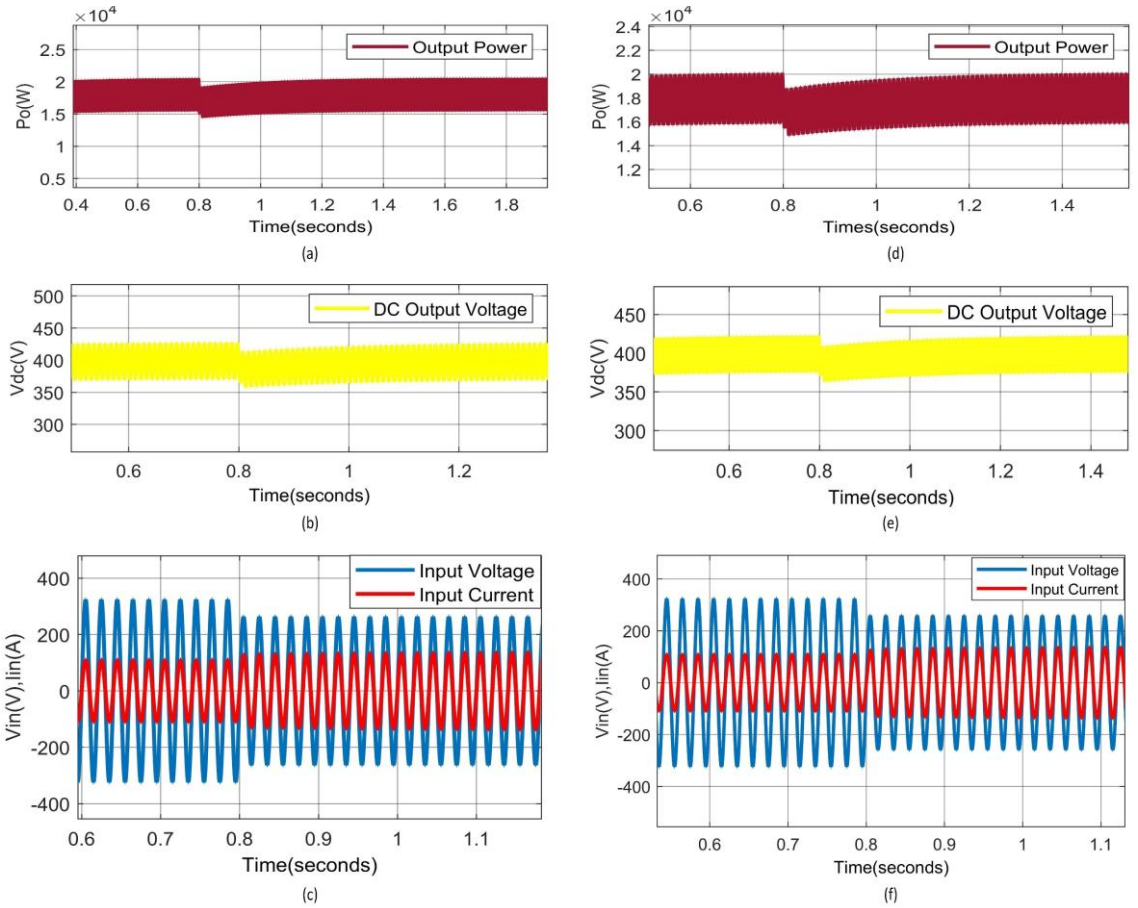

Figure 7. Dynamic Behavior waveforms during voltage sag. (a-c) Totem-Pole Prototype. (d-f) Interleaved Totem-Pole Prototype.

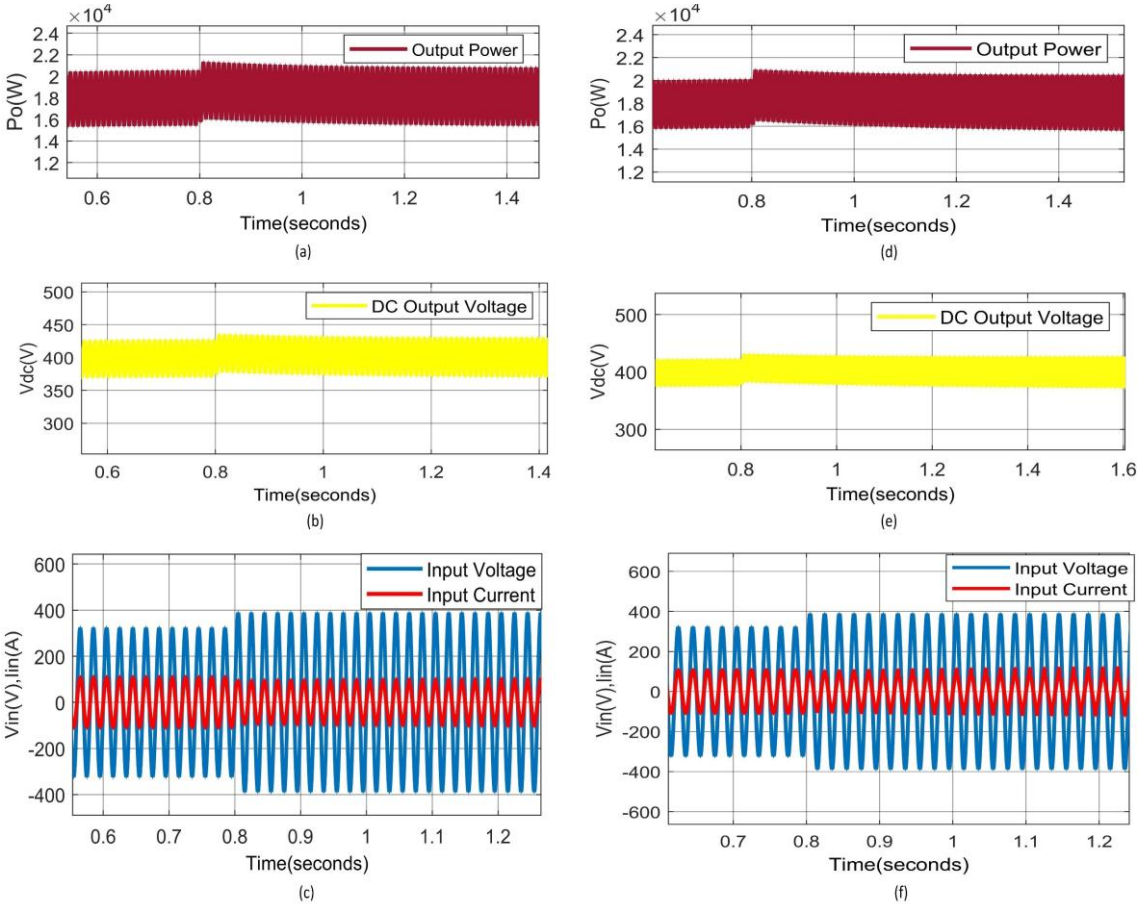

Figure 8. Dynamic Behavior waveforms during voltage swell. (a-c) Totem-Pole Prototype. (d-f) Interleaved Totem-Pole Prototype.

The interleaved architecture enhances stability by distributing current across both phases, which increases the converter's resilience to fluctuations in input voltage.

The results for the interleaved totem-pole prototype demonstrate that the response time for voltage sag ranges from 0.5 to 0.6 seconds in the worst-case scenario. The THD of the source current for the totem-pole configuration is 2.32%, whereas the interleaved topology achieved a slightly lower THD of 2.29%. This small improvement reflects the benefit of interleaving in reducing input current ripple and harmonics. Both values comply with IEEE 519 standards, confirming that both topologies are suitable for grid-connected EV applications in terms of harmonic performance, as illustrated in Figure 9 (a) and (b).

In the second dynamic scenario, a 20% input voltage swell was applied at t = 0.8 s, increasing the AC input from 230 Vrms to 276 Vrms under a fixed output power of 18 kW. The simulation results, shown in Figure 8, capture the converters' transient responses to this overvoltage case. Both converters exhibited a slight increase in the output DC-link voltage and output power at t = 0.8 s, as shown in Figures 8(a) and 8(b) for the totem-pole converter, and in Figures 8(d) and 8(e) for the interleaved totem-pole converter. Although these values increased slightly, they remained within the permissible operational limits.

Moreover, under varying output voltage and power demand conditions, both prototypes maintained a high PF, as evidenced by the input current waveforms shown in Figures 8(c) and 8(f). This behavior can be attributed to the outer voltage loop of the controllers, which effectively responded by decreasing the I_{ref} drawn from the source, as depicted in the aforementioned figures. This behavior confirms that both converter designs can withstand grid overvoltage conditions without compromising power quality.

Under voltage swell conditions, the THD of the source current increased significantly for both converters. As illustrated in Figure 9(c), the totem-pole converter recorded a THD of 9.49%, while the interleaved version had a higher THD of 19.9% as shown in Figure 9(d). Both values exceed the IEEE 519 recommended limit of 5% for grid-connected applications, indicating that the converters operate outside their optimal range during extreme overvoltage. However, when tested at a slightly lower swell level of 270 Vrms, both converters maintained a THD below 5%, which is consistent with typical residential grid tolerances. This suggests that the proposed topologies are suitable for practical grid conditions, but may require additional harmonic mitigation or improved control strategies for more severe swell events.

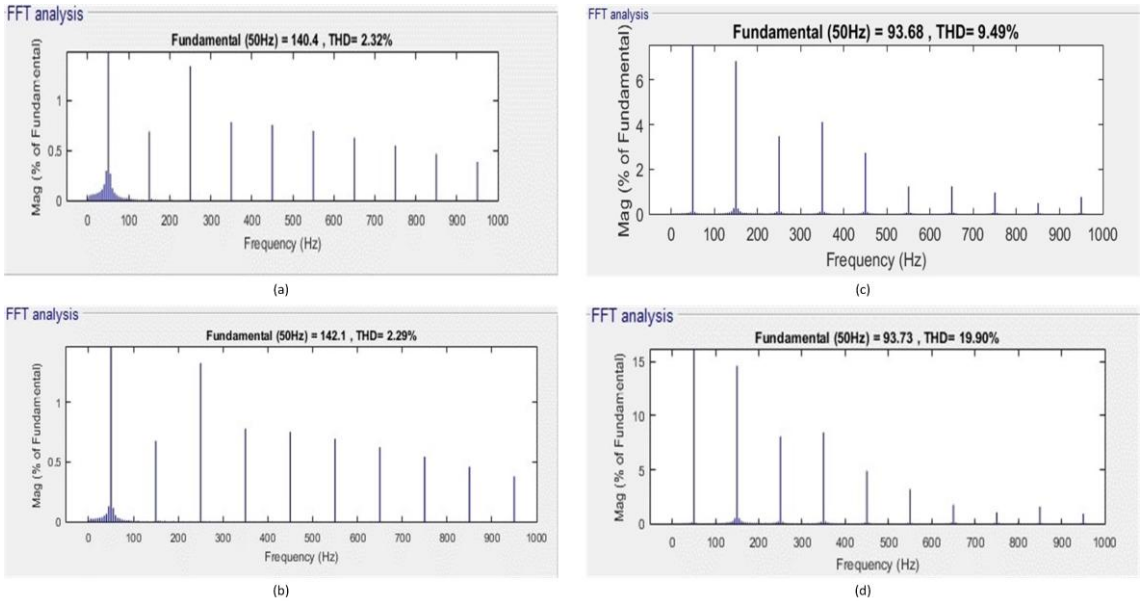

Figure 9. THD spectra of the source current under dynamic conditions. (a) and (b) show the THD at 184 Vrms input (voltage sag) for the totem-pole and interleaved totem-pole converters, respectively. (c) and (d) illustrate the THD at 276 Vrms input (voltage swell) for the same converter topologies.

4. Topologies Comparison

The comparative efficiency performance of the two converter topologies is illustrated in Figure 10. Both the bidirectional totem-pole and the interleaved totem-pole converters demonstrate high efficiency across a wide power range, particularly under mid-to-high load conditions. The interleaved topology consistently outperforms the standard totem-pole configuration when

the output power exceeds 10 kW. This is primarily due to better current distribution across parallel switching legs, which reduces conduction losses. However, at low power levels (below ~1 kW), both converters exhibit noticeable efficiency degradation, making them less suitable for light-load conditions. In such scenarios, conventional bridgeless or bridge PFC topologies may offer superior performance with lower switching losses.

Figures 11 and 12 illustrate the THD of the source current throughout the entire power range for both converter topologies. The results show that both converters maintain THD levels below the 5% threshold established by the IEEE 519 standard under steady-state conditions.

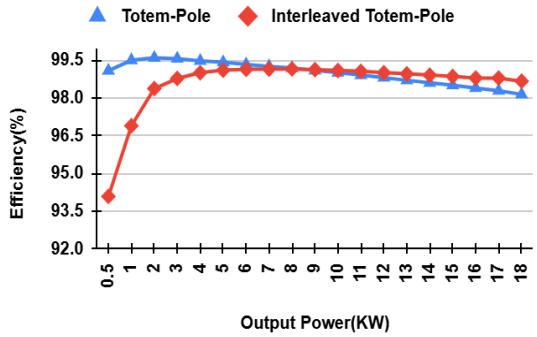

Figure 10. Efficiency versus output power for two totem pole PFC converters.

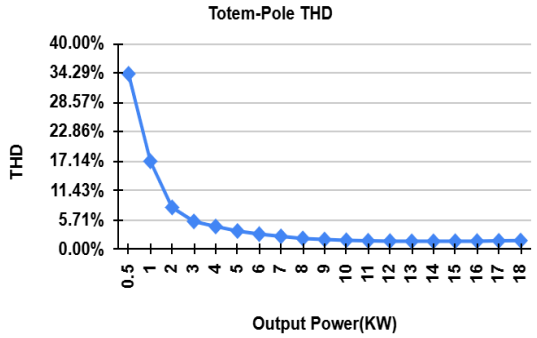

Figure 11. THD as a function of output power for Totem-Pole Topology.

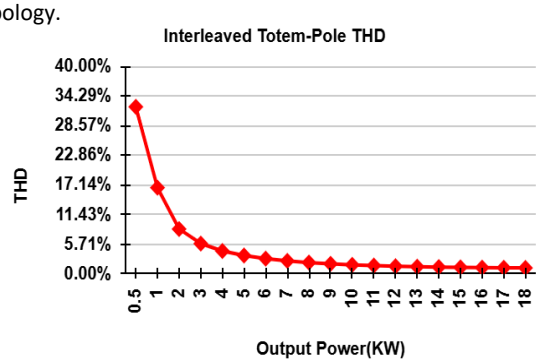

Figure 12. THD as a function of output power for Interleaved Totem-Pole Topology.

Notably, the interleaved topology exhibits slightly lower THD across most power levels, particularly at higher loads, due to its reduced input current ripple and the phase cancellation effect. This supports the suitability of both designs for grid-connected EV applications, with the interleaved version demonstrating marginally better harmonic performance.

Across the full load range (500 W-18 kW), both topologies maintained a power factor of 0.999, indicating lower input current distortion and minimal phase displacement between input voltage and current. This reinforces the effectiveness of the average current control strategy in achieving near-unity power factor performance.

The proposed totem-pole and interleaved totem-pole topologies achieve a lower THD compared to the 7.7 kW bidirectional converter discussed in (Kumar and Yi 2022). Specifically, the proposed topologies attain THD values of 1.72% and 1.14%, respectively, at a higher power level of 18 kW. In contrast, the THD during Grid-to-Vehicle (G2V) operation was 4.81%. Additionally, these new topologies demonstrate reduced THD at the same rated power, showing improved scalability. Similarity, while (Tang, Ding, and Khaligh 2016) proposed a 3.3 kW interleaved bridgeless totem-pole PFC converter for plug-in electric vehicles, achieving a maximum efficiency of 98.9% and a THD of 2.78% at 2KW power rating using SiC-based switches with regulated dc-link voltage in range 300V to 600V. While the proposed interleaved totem pole has less THD and efficiency at 2KW, it offers enhanced power handling capability and an expanded regulated output voltage range of 350 V to 800 V.

The main disadvantage of the proposed topologies is the high output ripple that occurs as the output power capability of the converters increases. In the worst-case scenario, this ripple can reach around 50V, which poses a limitation for selecting these types of PFC converters in high-power applications. The simulation results show that the totem pole topology has less output ripple compared to the interleaved topology. Therefore, the choice between the two topologies of the totem pole PFC converter ultimately depends on the specific input and output requirements, which will determine both the cost and size of the converter.

5. Conclusion

This research examined two single-phase totem-pole PFC converter topologies: the bidirectional and the bidirectional interleaved designs. The goal was to evaluate their effectiveness in improving power quality for Level 2 bidirectional EV chargers, with a power range extending up to 18 kW. Both converters demonstrated excellent performance, achieving a near-unity power factor of 0.999 and adhering to IEEE 519 standard for THD across a broad operating range. The interleaved topology showed higher efficiency and better THD performance,

especially at power levels exceeding 10 kW, making it more suitable for high-power applications. However, this configuration also exhibited greater output voltage ripple compared to the standard totem-pole topology, which could restrict its use in applications that require low ripple. The study emphasizes that the choice between these topologies should be based on specific application requirements, such as output ripple tolerance, efficiency, and power quality needs. Future work may investigate advanced control strategies and design of passive components to reduce the ripple issues encountered during high-power operations.

Declaration of Ethical Standards
The authors declare that they comply with all ethical standards.

Declaration of Ethical Standards
The authors declare that they comply with all ethical standards.

Credit Authorship Contribution Statement
Author-1: Conceptualization, investigation, methodology and software, visualization and writing – original draft.
Author-2: Conceptualization, supervision – review and editing.

Declaration of Competing Interest
The authors have no conflicts of interest to declare regarding the content of this article.

Data Availability Statement
The authors declare that the main data supporting the findings of this work are available within the article.

6. References

Adiga, P. S., Iyer, S. R., Dsouza, R. C., Kumar, H., Arjun, M., and Venkatesaperumal, B., (2022). A PFC hysteresis current controller for totem-pole bridgeless bi-directional EV charger. *IEEE International Conference on Power Electronics, Smart Grid, and Renewable Energy (PESGRE)*, Trivandrum, India, pp. 1-4, 2022, IEEE. https://doi.org/10.1109/PESGRE52268.2022.9715845

Alsalemi, Abdulazeez, and Ahmed Massoud., (2024). Effortless Totem-Pole Converter Control Using a Power Factor Correction Peak Current-Mode Controller. *Sensors*, 24, **15**, 4910. https://doi.org/10.3390/S24154910/S1

Dominic, L. B., Saju, B., Cleetus, J. M., Varghese, A., and Abraham, C., (2024). Review of Totem-Pole Boost Bridgeless PFC Rectifier Intended for On-Board EV Charging. *1st International Conference on Trends in Engineering Systems and Technologies (ICTEST)*, Kochi, India, pp. 01-06, 2024, IEEE. https://doi.org/10.1109/ICTEST60614.2024.10576074

Figueiredo, J. P. M., Tofoli, F. L., and Silva, B. L. A. A Review of Single-Phase PFC Topologies Based on the Boost Converter. *9th IEEE/IAS International Conference on Industry Applications-INDUSCON 2010*, Sao Paulo, Brazil, pp. 1-6, 2010, IEEE. https://doi.org/10.1109/INDUSCON.2010.5740015

Ghosh, S., Hu, Y., and Batarseh, I., (2023) . Review of Totem Pole PFC Soft-Switching Methods with Market Survey. *IEEE Energy Conversion Congress and Exposition (ECCE)*, Nashville, TN, USA, pp. 2891-2895, 2023, IEEE. https://doi.org/10.1109/ECCE53617.2023.10362518

Gupta, S., and Kumar, V. V., (2023).Performance analysis and loss estimation of an AC-DC PFC topologies of an EV charger. *2023 International Conference on Power, Instrumentation, Energy and Control (PIECON)*, Aligarh, India, pp. 1-6, 2023, IEEE. https://doi.org/10.1109/PIECON56912.2023.10085786

Huang, A. Q., (2016). Wide bandgap (WBG) power devices and their impacts on power delivery systems. *2016 IEEE International Electron Devices Meeting (IEDM)*, San Francisco, CA, USA, pp. 20.1.1-20.1.4, 2016, IEEE. https://doi.org/10.1109/IEDM.2016.7838457

Huber, L., Jang, Y., and Jovanovic, M. M., (2008). Performance evaluation of bridgeless PFC boost rectifiers. in *IEEE Transactions on Power Electronics*, vol. 23, **3**, pp. 1381-1390, May 2008, IEEE. https://doi.org/10.1109/TPEL.2008.921107

Mussa, S. A., and Jappe, T. K., (2009). Current control techniques applied in PFC boost converter at instantaneous power interruption. *2009 35th Annual Conference of IEEE Industrial Electronics*, Porto, Portugal, pp. 346-351, 2009, IEEE. https://doi.org/10.1109/IECON.2009.5414946

Kong, P., Wang, S., and Lee, F. C., (2007). Common mode EMI noise suppression in bridgeless boost PFC converter. *APEC 07 - Twenty-Second Annual IEEE Applied Power Electronics Conference and Exposition*, Anaheim, CA, USA, pp. 929-935, 2007, IEEE. https://doi.org/10.1109/APEX.2007.357626

Kumar, V., and Yi, K., (2022). Single-phase, bidirectional, 7.7 kW totem pole on-board charging/discharging infrastructure. *Applied Sciences*, *12*, **4**, 2236. https://doi.org/10.3390/app12042236

Li, X., and Niu, P., (2024). Research on Totem-Pole Power Factor Correction Based on Sliding Mode Control. *2024 4th International Conference on Energy Engineering and Power Systems (EEPS)*, Hangzhou, China, pp. 1196-1200, 2024, IEEE. https://doi.org/10.1109/EEPS63402.2024.10804283

Liu, Z., Lee, F. C., Li, Q., and Yang, Y., (2016). Design of GaN-based MHz totem-pole PFC rectifier. İn *IEEE Journal of Emerging and Selected Topics in Power Electronics*, vol. 4, **3**, pp. 799-807. https://doi.org/10.1109/JESTPE.2016.2571299

Lu, B., Brown, R., and Soldano, M., (2005). Bridgeless PFC implementation using one cycle control technique. *Twentieth Annual IEEE Applied Power Electronics Conference and Exposition, 2005. APEC 2005.*, Austin, TX, USA, pp. 812-817, 2005, IEEE. https://doi.org/10.1109/APEC.2005.1453073

Metwly, M. Y., Abdel-Majeed, M. S., Abdel-Khalik, A. S., Hamdy, R. A., Hamad, M. S., and Ahmed, S., (2020). A review of integrated on-board EV battery chargers: Advanced topologies, recent developments and optimal selection of FSCW slot/pole combination. *IEEE Access*, vol. 8, pp. 85216-85242. https://doi.org/10.1109/ACCESS.2020.2992741

Musavi, F., Eberle, W., and Dunford, W. G., (2011). A phase shifted semi-bridgeless boost power factor corrected converter for plug in hybrid electric vehicle battery chargers. *2011 Twenty-Sixth Annual IEEE Applied Power Electronics Conference and Exposition (APEC)*, Fort Worth, TX, USA, pp. 821-828, 2011, IEEE. https://doi.org/10.1109/APEC.2011.5744690

Park, M. H., Baek, J., Jeong, Y., and Moon, G. W., (2019). An interleaved totem-pole bridgeless boost PFC converter with soft-switching capability adopting phase-shifting control. *IEEE Transactions on Power Electronics*, vol. 34, **11**, pp. 10610-10618. https://doi.org/10.1109/TPEL.2019.2900342

Prídala, M., Šupolík, M., and Praženica, M., (2025). Design and Verification of a Bridgeless Totem-Pole Power Factor Corrector. Electronics, 14, **2**, 226. https://doi.org/10.3390/ELECTRONICS14020226

Safayatullah, M., Elrais, M. T., Ghosh, S., Rezaii, R., and Batarseh, I., (2022). A comprehensive review of power converter topologies and control methods for electric vehicle fast charging applications. *IEEE Access*, vol. 10, pp. 40753-40793, 2022, IEEE. https://doi.org/10.1109/ACCESS.2022.3166935

Sayed, M. A., Suzuki, K., Takeshita, T., and Kitagawa, W., (2017). PWM switching technique for three-phase bidirectional grid-tie DC–AC–AC converter with high-frequency isolation. *IEEE Transactions on Power Electronics*, vol. 33, **1**, pp. 845-858, Jan. 2018, IEEE. https://doi.org/10.1109/TPEL.2017.2668441

Singh, A., and Tiwari, A. N., (2020). Analysis of Bridge and Bridgeless type PFC AC-DC Boost Converter. *2020 International Conference on Electrical and Electronics Engineering (ICE3)*, Gorakhpur, India, , pp. 178-183, 2020, IEEE. https://doi.org/10.1109/ICE348803.2020.9122893

Su, B., and Lu, Z., (2010). An interleaved totem-pole boost bridgeless rectifier with reduced reverse-recovery problems for power factor correction. *IEEE Transactions on Power Electronics*, vol. 25, **6**, pp. 1406-1415. https://doi.org/10.1109/TPEL.2010.2040633

Reddy, M. S., Kumar, R., Saddriwala, M. A., and Alam, M., (2024). Design and analysis of bidirectional totem pole pfc rectifier for battery charging applications. *2024 IEEE Students Conference on Engineering and Systems (SCES)*, Prayagraj, India, pp. 1-6, 2024, IEEE. https://doi.org/10.1109/SCES61914.2024.10652394

Tang, Y., Ding, W., and Khaligh, A., (2016). A bridgeless totem-pole interleaved PFC converter for plug-in electric vehicles. *2016 IEEE Applied Power Electronics Conference and Exposition (APEC)*, Long Beach, CA, USA, pp. 440-445, 2016, IEEE. https://doi.org/10.1109/APEC.2016.7467909

Upputuri, R. P., and Subudhi, B., (2023). A comprehensive review and performance evaluation of bidirectional charger topologies for V2G/G2V operations in EV applications. *IEEE Transactions on Transportation Electrification*, vol. 10, **1**, pp. 583-595. https://doi.org/10.1109/TTE.2023.3289965

Ye, H., Yang, Z., Dai, J., Yan, C., Xin, X., and Ying, J., (2004). Common mode noise modeling and analysis of dual boost PFC circuit. *INTELEC 2004. 26th Annual International Telecommunications Energy Conference*, Chicago, IL, USA, pp. 575-582, 2004, IEEE. https://doi.org/10.1109/INTLEC.2004.1401526

Yilmaz, M., and Krein, P. T., (2012). Review of battery charger topologies, charging power levels, and infrastructure for plug-in electric and hybrid vehicles. *IEEE Transactions on Power Electronics*, vol. 28, **5**, pp. 2151-2169. https://doi.org/10.1109/TPEL.2012.2212917

Zhou, L., Wu, Y., Honea, J., and Wang, Z., (2015). High-efficiency true bridgeless totem pole PFC based on GaN HEMT: Design challenges and cost-effective solution. *Proceedings of PCIM Europe 2015; International Exhibition and Conference for Power Electronics, Intelligent Motion, Renewable Energy and Energy Management*, Nuremberg, Germany, pp. 1-8, 2015, VDE.

Internet References

1- Chellappan, S., (2018). A comparative analysis of topologies for a bridgeless-boost PFC circuit. https://www.ti.com/lit/an/slyt750/slyt750.pdf (6.07.2025)
2- Botsford, Charles, and Adam Szczepanek., (2009). Fast Charging vs. Slow Charging: Pros and Cons for the New Age of Electric Vehicles. https://www.researchgate.net/publication/2289971

58_Fast_Charging_vs_Slow_Charging_Pros_and_cons_for_the_New_Age_of_Electric_Vehicles (6.07.2025)

3- Firmansyah, E., Tomioka, S., Abe, S., Shoyama, M., and Ninomiya, T., (2010). An Interleaved Totem-Pole Power Factor Correction Converter. https://www.researchgate.net/publication/45573039_An_Interleaved_TotemPole_Power_Factor_Correction_Converter (6.07.2025)
4- The Massachusetts Department of Energy Resources, (2014). INSTALLATION GUIDE FOR ELECTRIC VEHICLE SUPPLY EQUIPMENT (EVSE). https://www.mass.gov/doc/electric-vehicle-charging-infrastructure-manual/download (6.07.2025)